



City Research Online

City, University of London Institutional Repository

Citation: Chen, C-C. & Tyler, C. W. (2008). Spectral analysis of fMRI signal and noise. In: Onozuka, M. & Chen-Tung, Y. (Eds.), *Novel Trends in Brain Science*. (pp. 63-76). Japan: Springer Japan. ISBN 9784431732419 doi: 10.1007/978-4-431-73242-6_4

This is the accepted version of the paper.

This version of the publication may differ from the final published version.

Permanent repository link: <https://openaccess.city.ac.uk/id/eprint/7056/>

Link to published version: https://doi.org/10.1007/978-4-431-73242-6_4

Copyright: City Research Online aims to make research outputs of City, University of London available to a wider audience. Copyright and Moral Rights remain with the author(s) and/or copyright holders. URLs from City Research Online may be freely distributed and linked to.

Reuse: Copies of full items can be used for personal research or study, educational, or not-for-profit purposes without prior permission or charge. Provided that the authors, title and full bibliographic details are credited, a hyperlink and/or URL is given for the original metadata page and the content is not changed in any way.

City Research Online:

<http://openaccess.city.ac.uk/>

publications@city.ac.uk

Spectral Analysis of fMRI Signal and Noise

Chien-Chung Chen¹ and Christopher W. Tyler²

Summary

We analyzed the noise in functional magnetic resonance imaging (fMRI) scans of the human brain during rest. The noise spectrum in the cortex is well fitted by a model consisting of two additive components: flat-spectrum noise that is uniform throughout the MRI image and frequency-dependent biological noise that is localized to the neural tissue and declines from low to high temporal frequencies. We show that the frequency-dependent component is well fitted by the f^{-p} model with $0 < p < 1$ throughout the measured frequency range. The parameters of the model indicate that the characteristic noise is not attributable to the temporal filtering of the hemodynamic response but is an inherent property of the blood oxygenation level-dependent (BOLD) signal. We then analyzed the power spectrum of the BOLD signal for various cognitive tasks. The signal-to-noise ratio of a typical fMRI experiment peaks at around 0.04 Hz.

Key words Blood oxygenation level-dependent (BOLD), Rest scan, Cortex, Stochastic process

Introduction

In a typical functional magnetic resonance imaging (fMRI) experiment, the local change in blood oxygenation level-dependent (BOLD) activity in the brain of a participant over time was measured while the participant engaged in certain sensorimotor or cognitive tasks [1]. Using this technique, the relative activation in cortical regions on a spatial scale of millimeters of cortex can be compared for a wide variety of tasks designed to isolate aspects of neural function—from early sensory processing to complex decision making and action planning. One major limiting factor for fMRI is the low signal-to-noise ratio (SNR) of the BOLD

¹Department of Psychology, National Taiwan University, Taipei 106, Taiwan

²The Smith-Kettlewell Eye Research Institute, San Francisco, CA 94115, USA

activity. Here, “signal” means the BOLD activity driven by the psychological tasks designated by the experimenters, and “noise” means the activity unrelated to such tasks. In a typical fMRI experiment, hemodynamic modulation induced by a psychological task is about 1%–5% around the mean activation level. The random variation of the BOLD activation can easily reach 2%–4% in magnitude [2]. Thus, fMRI data analysis is highly susceptible to noise. The purpose of this study was to analyze both the signal and noise power spectra of BOLD activation during a typical fMRI experiment time course. This knowledge has implications for better fMRI experimental designs and data analysis.

Because the noise is defined as the BOLD activity in the brain unrelated to any specific psychological task designated by the experimenter, the noise spectrum can be measured with a rest scan—that is, when participants are not required to perform any task except close their eyes and remain still throughout a scan run. The Fourier transform of such rest scan time series measures the average power spectrum of BOLD noise. It is important to understand the properties of the noise spectra to optimize the design of the activation signals for a maximal SNR.

It has been shown that the power spectrum of BOLD noise in the brain decreases with temporal frequency [3–6]. In particular, Zarahn et al. [4] fitted the power spectrum with arbitrary expressions containing a negative slope of -1 and called it $1/f$ noise. Here we offer a more detailed analysis of the noise properties in various brain structures. First, one might expect that there would be an irreducible component of equipment noise in the magnetic resonance detection process, which is expected by default to be Gaussian white noise by virtue of its derivation from multiples sources in the measurement system. This white noise must be combined with a characteristic hemodynamic noise component with a negative slope set by the properties of the oxygen resonance in the magnetic field. It is not clear what aspect of the biological signal generates this negative slope.

We therefore analyzed the temporal frequency spectrum of the BOLD signal during rest scans in two ways. To isolate the nonbiological component, we characterized both the extracephalic fMRI spectrum for voxels selected from the space of the fMRI reconstruction lying outside the head and the spectrum for a water phantom. In the head, we segmented the voxels into those lying entirely within the cortical gray matter, those entirely within the white matter, those outside the brain, and a residual set on the basis of the mean BOLD level. As the cortical hemodynamic noise is most relevant for fMRI recording, we then characterized the (cortical) fMRI spectrum for gray matter voxels. For comparison, we also determined the fMRI spectrum for white matter voxels and extracephalic voxels.

The second approach was to analyze the slope of the noise power spectrum reflecting the stochastic process of the noise-generating mechanisms. At the two extremes, a flat spectrum of slope zero (“white noise”) is a characteristic of a memoryless stochastic process, and a slope of -1 is a result of a long-memory random walk process. The slope of the noise power spectrum thus reveals much information on the mechanisms of the noise that fMRI measures. We therefore fitted a multicomponent noise model to the data from rest scans.

The signal dynamics can be measured in both the frequency domain and the time domain. Bandettini [7] instructed his participants to move their fingers for a few seconds (on-epoch) and then rest for the same amount of time (off-epoch); they were then told to repeat the on-off switch several times. He showed that the BOLD activation change in the motor cortex between the on- and off-epochs increased with the period of on-off cycles. Boynton et al. [8] showed similar frequency-dependent activation change in the visual cortex to visual stimuli. In general, these power spectra showed a low pass characteristic.

In the time domain, the BOLD activation change following a brief psychological event is well known. The typical BOLD activation in the responsive cortical area shows an increase shortly after the stimulus onset and a post-stimulation undershoot after the stimulus offset [9, 10]. The duration of the activation increment depends on the stimulus duration. However, because the hemodynamic response is essentially linear under most circumstances [8], one can derive an empirical hemodynamic response function by deconvolving the activation time series and the sequence of stimulation [10] and, in turn, the power spectrum of the hemodynamic signal by its Fourier transform. Here we use the differential power spectrum of the fMRI signal to that of the noise to determine the temporal frequency of response with the best SNR. This result should help indicate the best time course for the fMRI experiments.

Noise

Spectra for Hardware Noise

We first investigated noise from nonbiological sources. Figure 1 shows the power spectrum of extracephalic voxels during rest scans. The time series contained 72

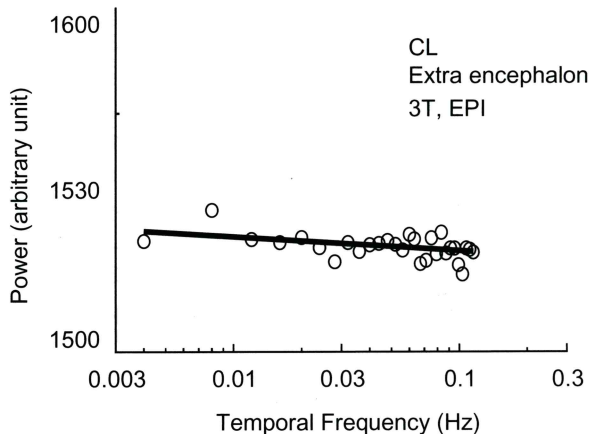


Fig. 1. Extracephalic resting spectra. Data show temporal frequency spectrum from voxels in the extracephalic space during the rest scan of observer C.L. Note that the functions are close to flat. *EPI*, echo planar imaging

volumes acquired with 3-s TR. The extracephalic voxels in the analysis were selected from a contiguous zone along the edges of the slice images. Those voxels were at least 30mm away from the closest encephalic voxels in the same-slice image. The time series data were acquired during a rest scan in eight participants. For images acquired with an echo planar imaging (EPI) sequence [11], we avoided choosing extracephalic voxels in the phase selection direction of the images to minimize the influence of ghost images. The mean intensity of extracephalic voxels was less than 10% of the mean intensity of the gray matter voxels (i.e., close to black in the images).

Figure 1 shows an example of the extraencephalic spectrum. The amplitude spectrum outside the brain is essentially flat up to the Nyquist frequency of 0.17Hz. For the fit of a straight line over the full spectrum in this log-log plot, the average slope for our eight participants was -0.04 ± 0.08 , showing no significant deviation from a white noise spectrum.

There is concern that the noise amplitude in a voxel increases with the mean intensity of that voxel. In this case, because the cephalic voxels have much higher intensity than the extracephalic voxels, the power spectra from extracephalic voxels may not reflect the full contribution of the hardware noise. Hence, we acquired data on water phantoms with the same time course as in the rest scan.

Although the mean intensity of the voxels in a water phantom was about 40 times the mean intensity of the extracephalic voxels in our scans, their power spectra showed similar behavior (Fig. 2). Across the spectrum, the average slope was 0.0007 ± 0.0027 for the two water phantom scans. This white noise behavior is expected from the prediction based on thermal and other noise sources in the scanner.

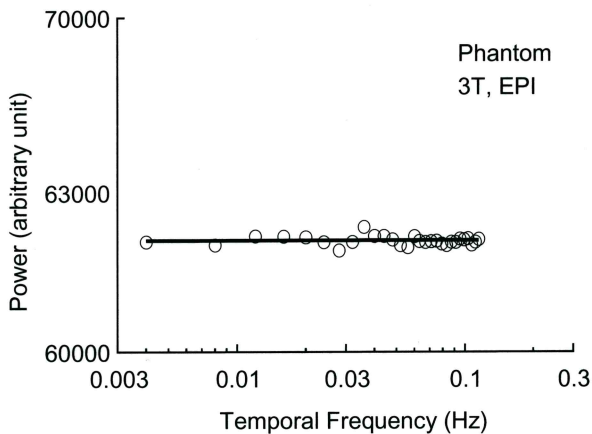


Fig. 2. Extracephalic resting spectrum. Data show temporal frequency spectrum from voxels in a water phantom. Note that the function is close to flat

Noise Spectra in the Brain

Figure 3 shows the power spectrum of time series data acquired in rest scans of eight participants. Six participants were scanned in the National Taiwan University magnetic resonance imaging/magnetic resonance spectroscopy (MRI/MRS) laboratory with an EPI sequence, and two participants were scanned in the Lucas Center of Stanford University with a spiral sequence. Because the participants were not required to perform any task during rest scans, the data acquired during such scans should be a good measurement of fMRI noise.

In contrast to the machine noise, the noise in the gray matter was typically maximum at the lowest measurable frequency (0.004 Hz) and declined progressively with the frequency, leveling out at higher frequencies. The decline with frequency is an important result because it implies that the noise-limiting BOLD signal becomes lower as the analysis frequency is increased, up to a certain value. The cortical noise amplitude is typically far larger than the extracephalic (hardware) noise at low temporal frequency. The difference can be as much as two log units, tending to converge at higher temporal frequencies. Note that this entire spectral range is well below 1 Hz, so we should not expect significant intrusion from heart pulses at ≥ 1 Hz. There might be some contamination from the respiration rate, however, because it should fall near 0.3 Hz. Nevertheless, we could not identify significant intrusion of cardiopneumatic noise, which would be realized as a spike in the power spectrum.

The noise characteristics specific to the cortex, or gray matter, may be compared with the results of the corresponding procedure after isolating the underlying white matter in the same regions of the brain during the same scans. The results (Fig. 4) are qualitatively similar to those for the cortex, seen in Fig. 3.

Because the noise spectrum is different inside and outside the head, it is evident that it consists of at least two components. We may analyze the component structure based on the simplifying assumption that there are two components that are additively independent: a component that derives from the dynamics of the BOLD activity (hemodynamic noise) and a component determined by thermal and other magnetic sources of noise in the scanner and its sensors (hardware noise). To obtain an uncontaminated estimate of the hemodynamic component of the noise, we make the assumption that the hardware noise component is uniform throughout the fMRI images (except in regions where ghost images from the head appear—any such regions were avoided for the extracephalic analysis). This assumption is justified by the flat spectrum for extracephalic noise and for the water phantom (Figs. 1, 2). Hence, the spectrum of the hardware noise should be $E(f) = h$, where h is a constant and f is the temporal frequency.

The cortical hemodynamic noise is assumed to have a uniform slope modeled by a power function $B(f) = bf^p$, where f is the frequency and p is the spectral slope. This power function corresponds to a straight line on a log-log plot and was termed a “1/f-like characteristic” by Bullmore et al. [5]. We assume that the hemodynamic noise and the hardware noise are independent from each other and combine by

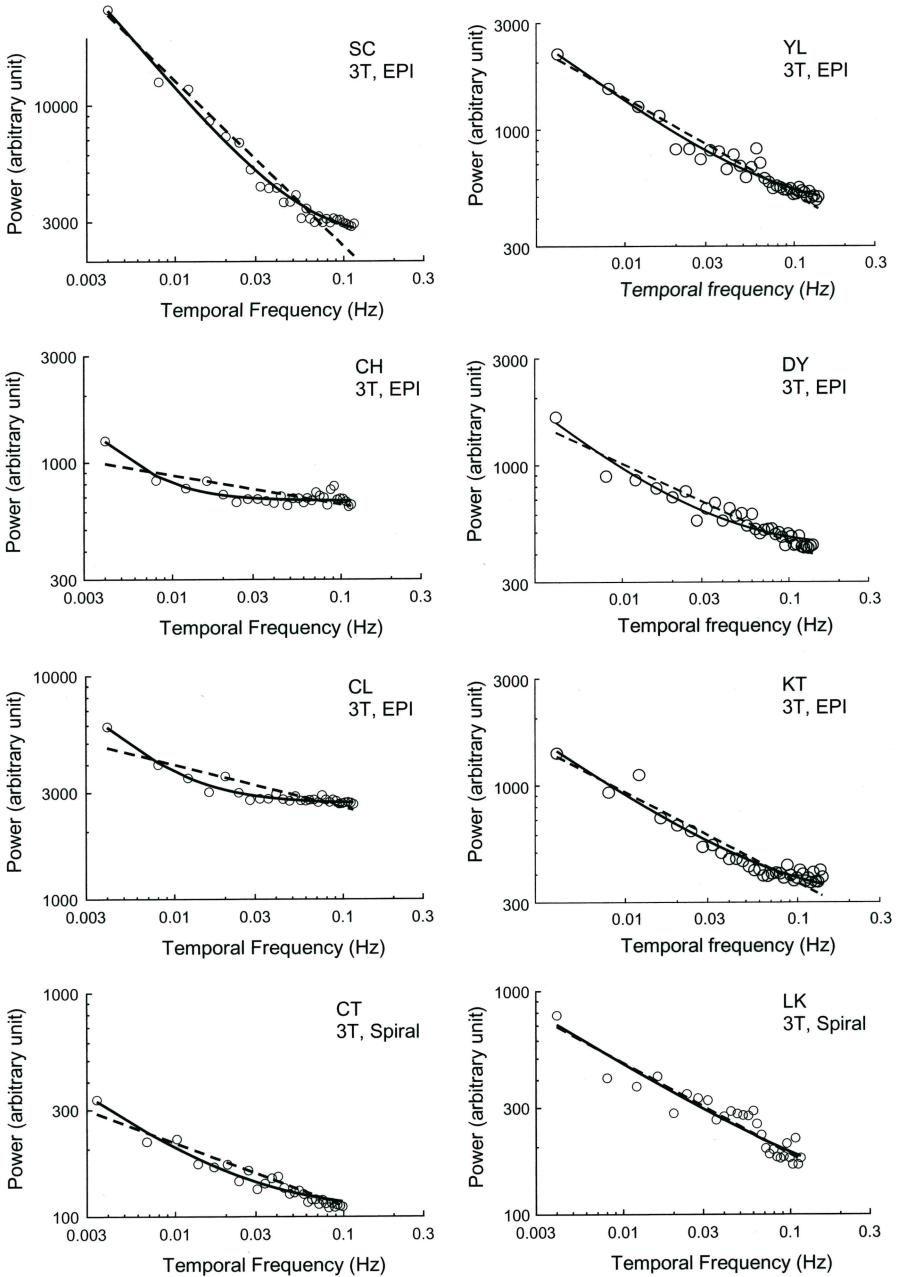


Fig. 3. Cortical resting spectra. Data show temporal frequency spectra from the gray matter of six observers. *Solid curve*, two-component model fits to the amplitude spectra. This model captures the systematic variation of the data over temporal frequency. *Dashed lines*, the $1/f$ -like function (f -p) fits

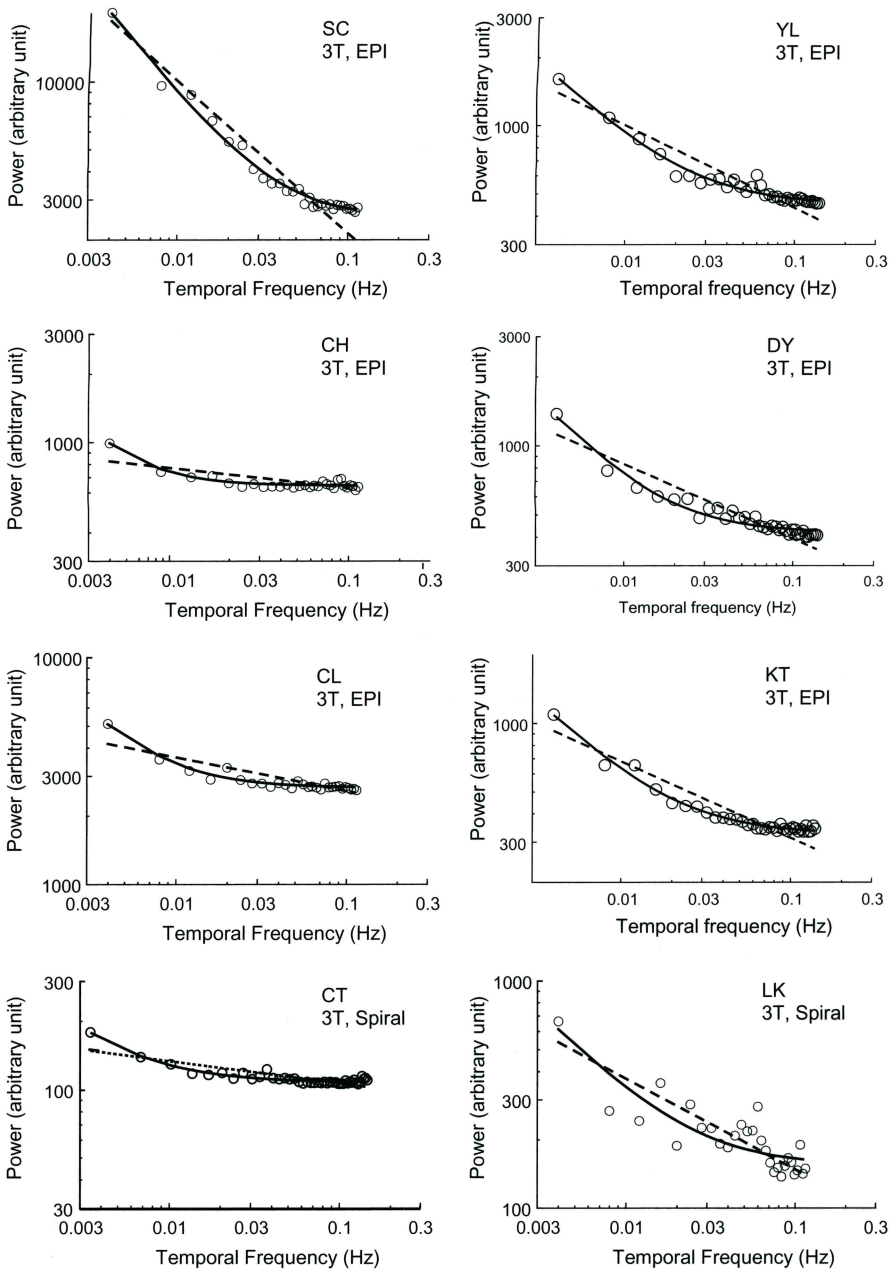


Fig. 4. White-matter resting spectra. Data are the temporal frequency spectra from white matter in the same scan. *Solid curve*, two-component model fits the amplitude spectra

adding their variances. Hence, in the cortex the noise spectrum, after the two sources combined, is

$$C(f) = [a \times E(f)^2 + b \times B(f)^2]^{0.5}$$

The fits for the two-component model are shown in Figs. 3 and 4 as the continuous curves for gray and white matter, respectively. The fit of this model is much better than 1/f-like noise alone (dashed lines in Figs. 3 and 4). On average, the sum-of-squares error (SSE) for the two-component model is three times better than that for the simple 1/f-like model for the gray matter and more than five times better for the white matter. Even considering the extra parameter, the reduction of SSE for the two-component model is highly significant: $F(8,414) = 46.72$ ($P < 0.0001$) for gray matter and $F(8,414) = 57.39$ ($P < 0.0001$) for white matter, pooled across participants. The slopes of the decreasing part of the spectrum varied from -0.45 to -0.92 across participants, with a mean of -0.65 ± 0.18 for gray matter and from -0.68 to -0.89 with a mean of -0.69 ± 0.25 for white matter. These slopes, which are not significantly different from one another, are about double those of the 1/f-like model fit, which has mean slopes of -0.36 ± 0.18 for gray matter and -0.30 ± 0.19 for white matter.

Mechanisms of Spectral Slopes

For the present data, the spectrum is almost flat at high temporal frequencies for most observers. This flat spectrum implies a white noise characteristic in this frequency region. In contrast to the random walk, which is a “long memory” process, white noise is memoryless. That is, the history of the noise-generating mechanism does not affect current responses. Our analysis supports the idea that the measured noise derives from a combination of a long-memory component and a memoryless component of the overall noise.

The major issue now becomes the interpretation of the hemodynamic component. The decrease in noise power with temporal frequency is reminiscent of what is commonly called “1/f noise” for the amplitude spectrum (which is the square of the amplitude spectrum), or “pink” noise. In fact, the average log–log slope for our data was -0.67 , somewhat shallower than the full 1/f property despite removal of the white noise component. For 1/f behavior of the amplitude spectrum, there are two classic explanations: random-walk behavior or white noise followed by a first-order filter. Random-walk behavior implies that the generating system randomly increases or decreases from its current position by a fixed amount during each (arbitrary) time interval. A random walk mechanism would have an unlimited 1/f spectrum down to whatever was the lowest measured frequency. The random walk is characteristic of increments governed by coin-flipping and of systems such as stock markets; and it is independent of the amplitude distribution governing the step size.

The other type of mechanism, the first-order filter, has asymptotic 1/f behavior for frequencies much higher than its corner frequency but an asymptotic slope of zero at low temporal frequencies. The only way to fit the present temporal spectra

with such a filter would be to assume that the f^{-p} slope was governed by a process whose “corner” fell in the range of the measured frequencies in Fig. 3, providing an empirical slope that was shallower than $1/f$. However, the data show no tendency to level off at the lowest frequency (0.004 Hz), so we assume that the relevant model for the physiological noise component is, in fact, the f^{-p} model.

Further analysis shows that the f^{-p} model of cortical BOLD noise is incompatible with the known blood dynamics in two ways. The blood dynamics relevant to the fMRI assay are characterized by the BOLD signal properties, which have been best analyzed by Buxton et al. [12] and Glover [10]. A representative fit of their models is a biphasic function with shallow resonance and a time constant of about 10 s. If this model characterizes the hemodynamic impulse response, it must necessarily be the filter that defines the hemodynamic limit on the noise spectrum (assuming that the noise generator has a flat spectrum). The frequency spectrum of such a hemodynamic filter model, as shown later, has a band-pass property that is obviously different from the noise spectrum. Zarahn et al. [4] made a similar point with respect to the $1/f$ fit to their data.

We therefore conclude that the most likely candidate to explain the hemodynamic noise spectrum is a separate f^{-p} property of the noise generation process rather than it being a reflection of the hemodynamic response properties. This separate noise generation process may operate through an extended series of filters or be a kind of constrained random walk process. Because the distribution on each voxel is accurately Gaussian [2], the falloff with frequency cannot be due to a nonlinearity in the amplitudes of the signal modulations but must be inherent in the time domain. At frequencies above about 1 Hz, this analysis suggests that the BOLD noise would conform to the f^{-p} property, flattening out when it reaches the level of the extracephalic noise. Our data suggest that the extracephalic-to-cortical noise ratio varies idiosyncratically among observers (Figs. 3, 4), so the frequency at which flattening occurs should also be idiosyncratic.

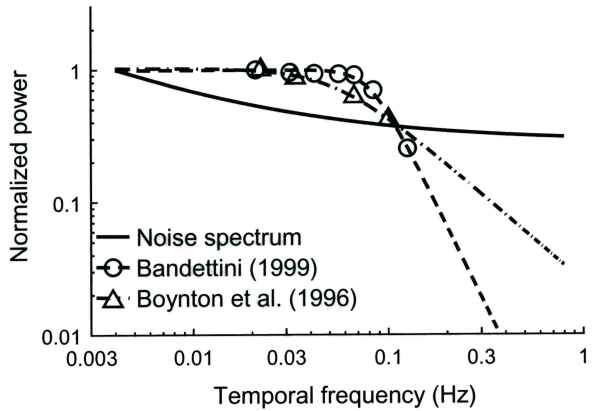
It is of interest that other aspects of brain processing also show a steep decline of noise amplitude with temporal frequency. Tyler et al. [13], for example, reported that the noise spectrum of the electrical brain activity fell with a log–log slope close to -1 over the range of 1–100 Hz. To the extent that both the scalp electrical potential and the BOLD hemodynamic response derive from slow electrochemical potentials in the neural cell bodies and their processes, it is not surprising to find a continuum of behavior in these activities. The implication of this joint result is that the neural potentials exhibit an approximation to $1/f$ behavior over more than a four-decade range of temporal frequencies, from 0.004 to 100 Hz.

Signal

Signal Spectrum

The signal spectrum of BOLD activation to certain sensorimotor or cognitive tasks may be obtained with a block design experiment. A typical block design fMRI

Fig. 5. Amplitude spectra for task-induced response in the motor (*open circles and dashed curve*) and the visual cortex (*open triangles and dash-dot curve*) and for the noise in the gray matter (*solid curve*)



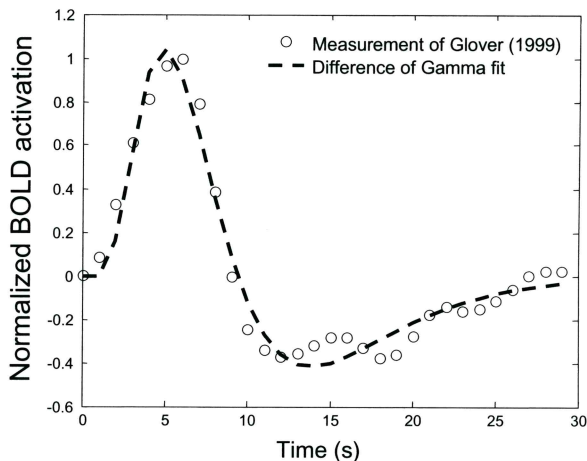
experiment has the participants alternately perform two tasks several times. The two tasks, ideally, differ in only one neuronal function. The experimenters then contrast the BOLD activation difference to these two tasks. If one systematically changes the temporal frequency of the alternation and observes how BOLD activation contrast changes with the temporal frequency, one can obtain the BOLD contrast sensitivity function (i.e., the BOLD contrast versus temporal frequency function) for the neuronal function in question.

Bandettini [7] measured the BOLD contrast sensitivity function for finger movement in the motor cortex. The BOLD contrast increases with the decrease of the temporal frequency. As shown in Fig. 5, we were able to fit a low-pass filter function (dashed curve) to his data (open circles). The data were derived from Bandettini's Figure 19.3 [7]. The noise spectrum (solid curve) is plotted in the figure as a comparison. The best-fitting filter function was second order (i.e., a two-pole filter). Boynton et al. [8] reported the BOLD contrast sensitivity function for viewing an 8-Hz counter-phase flickering checkerboard in the primary visual cortex. The open triangles in Fig. 5 were taken from the GMB data in Figure 6 of Boynton et al. [8]. Again, the BOLD contrast sensitivity function (dash-dot curve in Fig. 5) is well fit with a low-pass filter function. For these data, the best-fitting function was first order (i.e., a one-pole filter).

The hemodynamic response is essentially linear under most circumstances [8]. This implies that (1) the power spectrum of BOLD activation is the Fourier transform of the impulse response function [called hemodynamic response function (HRF) in this context] of the system; and (2) the fMRI time series is a convolution between HRF and the experimental sequence designated by the experimenter. These properties allow us to estimate the signal power spectrum from a vast body of time-domain data in the literature.

The shape of the hemodynamic response function is well known. Although there is disagreement about whether there is an initial dip 1–2 s [14] after the stimulus onset, it is generally agreed that the BOLD activation reaches its peak at around

Fig. 6. Difference of gamma fit to a hemodynamic response measured by Glover [10]



4–6s and is followed by a shallow undershoot that lasts up to 15–20s after the stimulus onset. The theoretical hemodynamic impulse response functions show a similar biphasic form [12, 15].

Figure 6 shows an example of the BOLD response after the onset of a short (1 s) auditory stimulus measured in the temporal cortex by Glover [10]. This function, we found, can be well fit by a difference of two gamma functions defined by

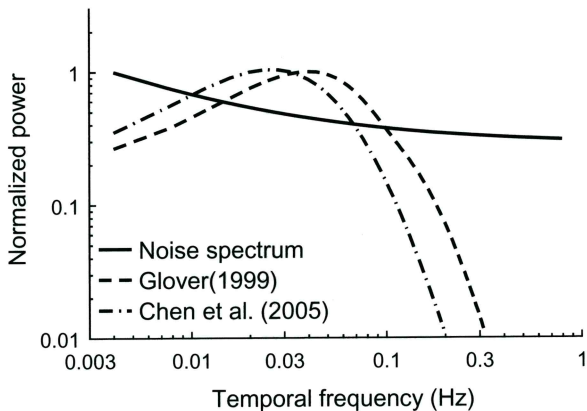
$$dg(x) = w_1 (x/\alpha_1)^{\beta_1} e^{-x/\alpha_1} - w_2 (x/\alpha_2)^{\beta_2} e^{-x/\alpha_2}$$

where w_i , α_i , and β_i , $i = 1, 2$ are free parameters. Among those parameters, α_i determines the position of the peak of the i -th component in time, β_i determines the steepness of response change in the i -th component, and w_i is a parameter of an arbitrary unit that determines the maximum response change of the i -th component.

As is shown by the smooth dashed curve in Fig. 6, this function incorporates sufficient parametrization to capture all the features of the responses [cf. 16]. We then Fourier-transformed this fitted response function to derive the predicted power spectrum of the BOLD activation as the dashed curve in Fig. 7. Again, the typical noise spectrum (solid curve) is plotted in the figure as a comparison. In contrast to the power spectrum obtained in the frequency domain, the signal power spectrum in the time domain shows a band-pass property with maximum power at 0.04 Hz.

The HRF can be derived by deconvolving the fMRI time series data and the stimulus sequence designated by the experimenter. Chen et al. [16] did this analysis for their visual experiment and fit the derived HRFs in the visual cortex with the difference in gamma functions. Here, we took the median of the difference in gamma parameters of the six participants in the study of Chen et al. [16] and computed a representative HRF of the visual cortex. We then Fourier-transformed this

Fig. 7. Amplitude spectra for task-induced response in the temporal cortex (*dashed curve*) and the visual cortex (*dash-dot curve*) and for the noise in the gray matter (*solid curve*)



fitted HRF to obtain the power spectrum of the BOLD activation as the dash-dot curve in Fig. 7. This curve also shows a band-pass property, with maximum power occurring at 0.032 Hz. This peak frequency corresponds to a 31-s period of task switching in a block design, or a 15.5-s epoch length. The power spectrum estimated from Glover [10] showed a peak frequency at 0.04 Hz, corresponding to a 12.5-s epoch length in a block design. The difference between the two studies, 3 s, is even smaller than the TR (repetition time) of the 3.5 s used by Chen et al. [16] and would not be detectable in most block design experiments.

There is also a discrepancy between the power spectra derived from the time domain studies (which show a band-pass property as in Fig. 7) and those directly measured in the frequency domain (which show a low-pass property as in Fig. 5). The band-pass property of the power spectrum is expected based on the fact that the HRF shows a biphasic shape, which implies attenuation of the system response to a longer stimulus and tuning to an optimal temporal frequency. The question is why the power spectrum measured in the frequency domain did not show attenuation at the low frequencies, implying a monophasic HRF. The reason of this discrepancy remains unresolved. One possible reason is that the undershoot is attributable to a nonlinearity in the system, such as recovery from early adaptation for long stimulation that is equated across frequency in the frequency measurement paradigm.

Signal-to-Noise Ratio

Although there are discrepancies in the signal power spectra from various studies, the signal-to-noise (SNR) shares largely similar properties. Figure 8 shows the typical SNR as a function of temporal frequency assuming the typical noise parameters derived from Fig. 3. The solid curve is the SNR computed by dividing the signal spectrum from the temporal cortex to an auditory stimulation [10]; the

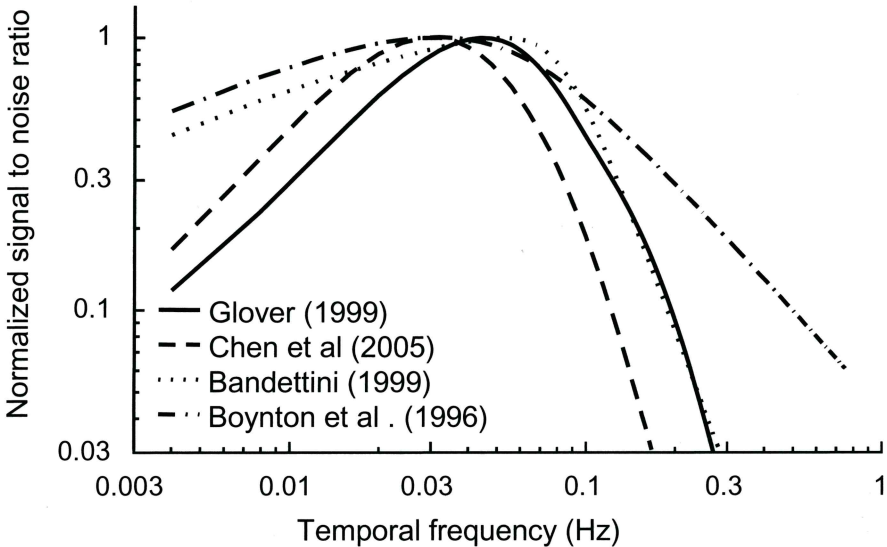


Fig. 8. Ratio of the task-induced response (signal) spectrum from four studies (see keys) and the noise spectrum

dashed curve, from the visual cortex to a visual stimulation [16]; the dotted curve, from the motor cortex during finger movement [7]; and the dash-dot curve, from the visual cortex to a visual stimulation [8]. Despite all these differences in brain areas and tasks, all the SNR curves show a band-pass property. The peak frequency ranges from 0.028 and 0.032 Hz in the two visual cortex studies [8, 16] to 0.04 Hz in the temporal cortex study [10] to 0.052 Hz in the motor cortex study [7]. This implies that, with a block design, a period of around 20–36 s or paired test and null epochs of 10–18 s should be the optimal stimulation rate.

Acknowledgments This work was supported by NIH/NEI grants 7890 and 13025 to C.W.T. and NSC grant 93-2752-002-H-007-PAE to C.C.C. Thanks go to Heidi Baseler for data collection of the spiral scans at Stanford University and to Chen Der-Yo and Liu Chia-Li for data collection of the spiral scans at National Taiwan University.

References

1. Ogawa S, Lee TM, Ray AR, et al (1990) Brain magnetic resonance imaging with contrast dependent on blood oxygenation. *Proc Natl Acad Sci USA* 87:9868–9872.
2. Chen CC, Tyler CW, Baseler HA (2003) The statistical properties of BOLD magnetic resonance activity in the human brain. *Neuroimage* 20:1096–1109.
3. Aguirre GK, Zarahn E, D'Esposito M (1997) Empirical analyses of BOLD fMRI statistics. II. Spatially smoothed data collected under null-hypothesis and experimental conditions. *Neuroimage* 5:199–212.

4. Zarahn E, Aguirre GK, D'Esposito M (1997) Empirical analyses of BOLD fMRI statistics. I. Spatially unsmoothed data collected under null-hypothesis conditions. *Neuroimage* 5:179–197.
5. Bullmore E, Long C, Suckling J, et al (2001) Colored noise and computational inference in neurophysiological (fMRI) time series analysis: resampling methods in time and wavelet domains. *Hum Brain Mapp* 12:61–78.
6. Pfeuffer J, Van de Moortele PF, Ugurbil K, et al (2002) Correction of physiologically induced global off-resonance effects in dynamic echo-planar and spiral functional imaging. *Magn Reson Med* 47:344–353.
7. Bandettini PA (1999) The temporal resolution of functional MRI. In: Moonen CTW, Bandettini PA (eds) *Functional MRI*. Springer, Heidelberg, pp 205–220.
8. Boynton GM, Engel SA, Glover GH, Heeger DJ (1996) Linear systems analysis of functional magnetic resonance imaging in human V1. *J Neurosci* 16:4207–4221.
9. Kwong KK, Belliveau JW, Chesler DA, et al (1992) Dynamic magnetic resonance imaging of human brain activity during primary sensory stimulation. *Proc Natl Acad Sci USA* 89: 5675–5679.
10. Glover GH (1999) Deconvolution of impulse response in event-related BOLD fMRI. *Neuroimage* 9:416–429.
11. Stehling MK, Turner R, Mansfield P (1991). Echo-planar imaging: magnetic resonance imaging in a fraction of a second. *Science* 254:43–50.
12. Buxton RB, Wong EC, Frank LR (1998) Dynamics of blood flow and oxygenation changes during brain activation: the balloon model. *Magn Reson Med* 39:855–864.
13. Tyler CW, Apkarian P, Nakayama K (1978) Multiple spatial-frequency tuning of electrical responses from human visual cortex. *Exp Brain Res* 33:535–550.
14. Hu X, Le TH, Ugurbil K (1997) Evaluation of the early response in fMRI in individual subjects using short stimulus duration. *Magn Reson Med* 37:877–884.
15. Aubert A, Costalat R (2002) A model of the coupling between brain electrical activity, metabolism, and hemodynamics: application to the interpretation of functional neuroimaging. *Neuroimage* 17:1162–1181.
16. Chen CC, Tyler CW, Liu CL, et al (2005) Lateral modulation of BOLD activation in unstimulated regions of the human visual cortex. *Neuroimage* 24:802–809.